Goda, K.; Ottaway, David John; Connelly, Blair; Adhikari, R.; Mavalvala, N.; Gretarsson, A M.. Frequency-resolving spatiotemporal wave-front sensor, *Optics Letters*, 2004; 29 (13):1452-1454.

Frequency-resolving spatiotemporal wave-front sensor

Keisuke Goda, David Ottaway, Blair Connelly, Rana Adhikari, and Nergis Mavalvala

LIGO Laboratory, Massachusetts Institute of Technology, NW17-161, Cambridge, Massachusetts 02139

Andri Gretarsson

LIGO Livingston Observatory, P.O. Box 940, Livingston, Louisiana 70754

Received February 20, 2004

We report on a high-resolution wave-front sensor that measures the complete spatial profile of any frequency component of a laser field containing multiple frequencies. This probe technique was developed to address the necessity of measuring the spatial overlap of the carrier field with each sideband component of the field exiting the output port of a gravitational-wave interferometer. We present the results of an experimental test of the probe, where we were able to construct the spatial profile of a single radio-frequency sideband at the level of −50 dBc. © 2004 Optical Society of America

OCIS codes: 040.2840, 120.5050, 120.2230, 140.4780, 100.5070, 110.2970.

A variety of wave-front sensing techniques for spatial profiling of laser beams exist.[1] Shack–Hartmann detectors,[2] for example, provide high spatial resolution, and heterodyne techniques[3–5] afford high sensitivity to lower-order spatial modes of the laser field with specific symmetries. None of these techniques, however, addresses the need for spatial profiling of a single-frequency component of a laser field, e.g., the sidebands of phase-modulated (PM) laser light. We describe a technique that constructs the spatial wave front of a radio-frequency (RF) sideband of PM laser light and present an experimental demonstration. The development of this technique was motivated by the need to separately measure the spatial modes of the carrier and PM sidebands exiting the output ports of a gravitational-wave interferometer, where different frequency components of the PM light that are incident upon the interferometer experience different spatial filtering.

Many gravitational-wave interferometers, e.g., the Laser Interferometer Gravitational-Wave Observatory (LIGO) detectors, comprise a Michelson interferometer with kilometer-long Fabry–Perot cavities in each arm and a several-meters-long power-recycling cavity at the input.[6] Interferometric signals are used to hold all three cavities on resonance and the Michelson interferometer on the dark fringe. Discriminants for these interferometer lengths, as well as for mirror misalignments, are derived by injecting PM light into the interferometer. The optical signals at the output ports are measured by heterodyne detection: RF phase modulation sidebands beat with carrier light.[7] The carrier is resonant in the arm cavities, which have g parameters[8] of ~0.33 and are effective spatial filters. The RF sideband fields, however, resonate only in the power-recycling cavity, which is nearly degenerate with a g parameter of ~1, and do not experience any significant spatial filtering. Moreover, the RF sidebands are significantly more sensitive to misalignments or other spatial distortions of the power-recycling cavity than the carrier field.[9] Consequently, the spatial modes of the carrier and RF sideband fields exiting the interferometer may be quite different. Maximum signal sensitivity requires perfect spatial overlap between the transverse modes of the carrier and RF sidebands. It is, therefore, desirable to measure the spatial mode of the RF sideband field independent of the carrier field. Furthermore, before the detector is fully optimized the RF sideband fields at frequencies above and below the carrier frequency, referred to as the upper and lower sideband, respectively, can experience different spatial distortions,[10] and knowledge of the spatial profiles of the upper and lower sidebands circulating in various parts of the interferometer is expected to be a valuable tool in optimizing the sensitivity of the detectors.

The basic principle behind the wave-front-sensing technique that we report here is to measure the beat note between the test laser and a reference laser that spatially overlaps it. Our wave-front sensor has two distinct properties: (i) high spatial resolution and (ii) frequency discrimination. The high spatial resolution is achieved by use of a reference field with high modal purity for interference with the test laser beam, as well as a high-spatial-resolution scan. A relatively fast (up to 10 Hz) scan rate is achieved, which is necessary to measure profiles faster than the dominant angular pointing fluctuations of the beams in the LIGO interferometers. Frequency discrimination is realized by heterodyne detection, which is used to measure the beat note between the reference laser and the frequency component of the test laser that is of interest.

The frequency discrimination is implemented by heterodyne detection but is distinct from previous heterodyne spatial profiling techniques.[4,5] Both these techniques are limited in the spatial resolution that can be obtained, and they cannot measure the spatial properties of the upper and lower sidebands independently, which is a key feature of our method.

To perform an experimental demonstration of this technique we constructed a benchtop experiment to measure the spatial amplitude and phase variation of a RF component of a PM test field. An important component of this experiment was the need to generate a test field similar to one that we might expect from a LIGO interferometer but with a controllable spatial

0146-9592/04/131452-03$15.00/0

mode. Our test field was generated by transmitting a RF sideband of the test laser in the Hermite–Gaussian TEM_{21} and TEM_{42} modes of a high-finesse cavity. We successfully reconstructed the frequency components in both the TEM_{21} and the TEM_{42} modes, the latter at a level of -50 dBc, with our wave-front sensor in the benchtop experiment. We recently installed a preliminary version of the wave-front sensor on a long-baseline gravitational-wave interferometer; that study will be reported in the future.

The experiment comprises two distinct parts: the wave-front sensor and the test field generator shown in the shaded boxes in Fig. 1. The test field generator was necessary just for the experimental test of the wave-front-sensing technique but is not part of the wave-front sensor itself.

The wave-front sensor reference laser beam was expanded by use of a two-lens telescope to give a fairly flat phase front at the photodetection plane. The reference field was interfered with the test field on the beam splitter. High-bandwidth photodiodes (PD2 and PD3) were used to measure the beat notes between the reference and the test lasers. Electronic filtering was used to eliminate the beats between the reference laser and other frequencies present in the test field. The light at one port (toward PD2) was used to track the time-dependent frequency difference between the two lasers, which was set by adjusting the frequency of the reference laser. Phase locking the two lasers was convenient but not essential. The light from the other port of the beam splitter was scanned across a 150-μm-diameter circular pinhole (PH) by use of galvanometers (GSI Lumonics Model 000-3008539) before it was detected by another high-bandwidth photodiode (PD3). The photocurrent from PD3 was demodulated in two orthogonal quadratures, and the spatial dependences of the I- and Q-phase voltages were used to obtain the amplitude and phase of the sideband. The spatial profiles of the phase and amplitude of the field were reconstructed from the measured RF signal by use of the expressions

$$|E(x,y)| = [V_I(x,y)^2 + V_Q(x,y)^2]^{1/2},$$

$$\phi(x,y) = \arg[V_I(x,y) + jV_Q(x,y)], \qquad (1)$$

where $V_I(x,y)$ and $V_Q(x,y)$ are the demodulated voltages in the I and Q phases, respectively, and x and y are the transverse coordinates of the beam.

PD3 measured the spatial content of the amplitude and phase of the combined field. To circumvent a scan rate limit resulting from the inertia of the galvanometers, a spiral pattern was chosen, as it permits a faster scan rate. We achieved a scan frequency of 5 Hz with a sampling rate of 1000 points per scan with no dwell time at each point. The limitation here was the sample rate of the data acquisition system used (National Instruments Model PCI 6052E).

The test field was the RF sideband of a second laser in a well-defined spatial mode. A low-power, monolithic Nd:YAG laser (Lightwave Model 120) was frequency locked to the TEM_{00} mode of a high-transmission, high-finesse, monolithic, standing-wave cavity with a free spectral range of 738.2 MHz. The frequency locking was done using the Pound–Drever–Hall technique[11] (with 13.3-MHz PM sidebands detected on PD1 and demodulated by mixer MX1). The test field was also PM at 81.9 MHz. The frequency of one of the 81.9-MHz sidebands was matched to the resonant frequency of a TEM_{21} mode of the reference cavity. The light field that was incident upon the monolithic cavity was deliberately mismatched to get appreciable overlap with the TEM_{21} mode of the cavity. Thus, the light exiting the cavity contained a carrier in the TEM_{00} mode along with a much smaller amplitude sideband in the TEM_{21} mode, separated from the carrier by 81.9 MHz. A RF sideband at twice the 81.9-MHz frequency also passed through the cavity in a TEM_{42} mode.

The frequency spectrum that was incident upon the wave-front sensor is shown in the gray box at the top left of Fig. 1. For our experiment the frequency of the reference laser was offset from one of the 81.9-MHz PM sidebands of the test field by 21.5 MHz. One can choose this frequency by sweeping of the reference laser frequency to coincide with any frequency component of the test field to be probed. The 21.5-MHz beat was detected on PD2 and demodulated with mixer MX2. The resulting discriminant was used for locking the reference laser frequency to that of the test laser. The same beat note at 21.5 MHz was also used as the local oscillator for demodulation of the wave-front-sensor signal on PD3. Since the dominant beat note in the RF spectrum was the beat between the reference and test laser carrier fields, it was necessary to bandpass filter the outputs of PD2 and PD3 such that only a band around 21.5 MHz remained in the photocurrent.

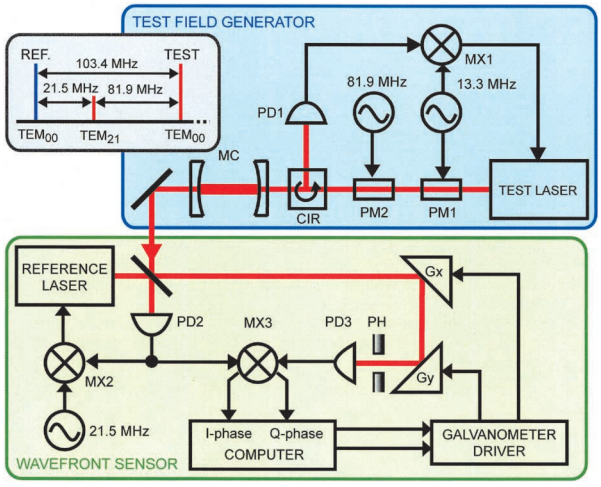

Fig. 1. Schematic of the experimental test of the wave-front sensor. The test field generator is shown in the blue box, and the wave-front sensor is shown in the green box. The gray box shows the spectrum of light that is incident upon the wave-front sensor; only the 21.5-MHz beat is detected with aggressive bandpass filtering. REF., reference field; MC, mode-cleaner cavity; CIR, circulator; PM1, PM2, phase modulators; Gx, Gy, galvanometers scanned in the x and y directions. Other abbreviations defined in text.

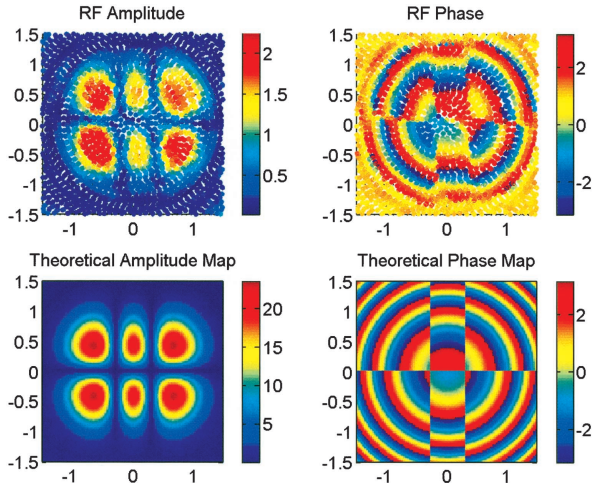

Fig. 2. Top maps: measured amplitude and phase of the first-order sideband in the TEM_{21} mode. Left, amplitude profile, color coded according to the bars at the right to show spatial variation in the relative amplitude. Right, phase profile, showing the sudden phase transitions that appear alternately as the amplitude changes polarity. Bottom maps: theoretical calculation of the amplitude and phase of the first-order sideband in the TEM_{21} mode, with color coding identical to that of the top maps and with no free parameters except an overall phase shift.

Measured maps of the spatial variation in the amplitude and phase of the first-order TEM_{21} sideband are shown at the top of Fig. 2. The amplitude plot clearly shows the six lobes that characterize a TEM_{21} mode, and the sudden phase transitions that appear alternately as the amplitude switches polarity are evident in the phase plot. These sharp phase transitions are superimposed on the gradual phase variation in the radial direction because of the spherical curvature of the TEM_{21} mode phase front. The power in the sideband was 40 times less than the carrier field during this experiment. Both maps show good qualitative agreement with the theoretical predictions illustrated at the bottom of Fig. 2.

Theoretical maps were generated by use of the exact optical parameters of the test and reference fields. The Hermite–Gaussian mode of the cavity through which the test field was transmitted overlapped the flat wave front of the reference field on the photodetector plane. The blurring of the sharp phase transitions in the center of the image is due to the limited isolation that the monolithic cavity provides for transmission of a TEM_{12} mode. The slight astigmatism of the cavity prevented complete degeneracy of the TEM_{21} and TEM_{12} modes; the best isolation that could be achieved was a reduction of 100 in power. Theoretical calculations clearly show this blurring of the phase transitions when a TEM_{12} of one-tenth the amplitude is added to a TEM_{21} mode. Although they are not shown, we also obtained clear images of a TEM_{42} mode with 300 times less power than the carrier power.

In summary, we have demonstrated a technique for spatial sensing of the wave front of a single-frequency component of a laser beam with high spatiotemporal resolution, obtaining the maps of the amplitude and the phase of the first- and second-order sidebands, which are much fainter than the carrier. The theoretical predictions are in good agreement with our experimental results. This is a powerful, noninvasive technique for analyzing the spatial behavior of any low-amplitude RF sideband without disturbing the carrier field. This wave-front sensor is currently being incorporated into the LIGO interferometers; results from a preliminary installation have already assisted in alignment and in measurement of the overlap of the carrier and RF sideband fields at the signal ports of the interferometer and will be reported in a subsequent work.

This research was supported by National Science Foundation grants PHY-9210038 and PHY-0107417. We gratefully acknowledge helpful comments from Peter Fritschel, David Shoemaker, and Mike Zucker. N. Mavalvala's e-mail address is nergis@mit.edu.

References

1. J. M. Geary, *Introduction to Wavefront Sensors*, Tutorial Text 18 (SPIE Press, Bellingham, Wash., 1995).
2. R. V. Shack and B. C. Platt, J. Opt. Soc. Am. **61,** 656 (1971) [abstract].
3. E. Morrison, B. J. Meers, D. I. Robertson, and H. Ward, Appl. Opt. **33,** 5037 (1994).
4. Y. Hefetz, N. Mavalvala, and D. Sigg, J. Opt. Soc. Am. B **14,** 1597 (1997).
5. G. Mueller, Q. Shu, R. Adhikari, D. B. Tanner, D. Reitze, D. Sigg, N. Mavalvala, and J. Camp, Opt. Lett. **25,** 266 (2000).
6. B. Barish and R. Weiss, Phys. Today **52**(10), 44 (1999).
7. P. Fritschel, R. Bork, G. González, N. Mavalvala, D. Ouimette, H. Rong, D. Sigg, and M. Zucker, Appl. Opt. **40,** 4988 (2001).
8. A. E. Siegman, *Lasers* (University Science, Mill Valley, Calif., 1986), p. 746.
9. P. Fritschel, N. Mavalvala, D. Shoemaker, D. Sigg, M. Zucker, and G. González, Appl. Opt. **37,** 6734 (1998).
10. E. D'Ambrosio and W. Kells, California Institute of Technology, MS18-34, Pasadena, California 91125 (personal communication, 2002).
11. R. W. P. Drever, J. L. Hall, F. V. Kowalski, J. Hough, G. M. Ford, A. J. Munley, and H. Ward, Appl. Phys. B **31,** 97 (1983).